Tissue-Engineered Articular Cartilage Exhibits Tension-Compression Nonlinearity Reminiscent of the Native Cartilage

Terri-Ann N. Kelly[1], **Brendan L. Roach**[1], **Zachary D. Weidner**[3], **Charles R. Mackenzie-Smith**[1], **Grace D. O'Connell**[1], **Eric G. Lima**[4], **Aaron M. Stoker**[5], **James L. Cook**[5], **Gerard A. Ateshian**[2], and **Clark T. Hung**[1,*]

[1]Cellular Engineering Laboratory, Department of Biomedical Engineering, Columbia University, New York, NY

[2]Musculoskeletal Biomechanics Laboratory, Departments of Biomedical and Mechanical Engineering, Columbia University, New York, NY

[3]Department of Orthopedic Surgery, St. Luke's-Roosevelt Hospital, New York, NY

[4]Open-Source Hardware Laboratory, Department of Mechanical Engineering, Cooper Union, New York, NY

[5]Comparative Orthopaedic Laboratory, College of Veterinary Medicine, University of Missouri, Columbia, MO

Abstract

The tensile modulus of articular cartilage is much larger than its compressive modulus. This tension-compression nonlinearity enhances interstitial fluid pressurization and decreases the frictional coefficient. The current set of studies examines the tensile and compressive properties of cylindrical chondrocyte-seeded agarose constructs over different developmental stages through a novel method that combines osmotic loading, video microscopy, and uniaxial unconfined compression testing. This method was previously used to examine tension-compression nonlinearity in native cartilage. Engineered cartilage, cultured under free-swelling (FS) or dynamically loaded (DL) conditions, was tested in unconfined compression in hypertonic and hypotonic salt solutions. The apparent equilibrium modulus decreased with increasing salt concentration, indicating that increasing the bath solution osmolarity shielded the fixed charges within the tissue, shifting the measured moduli along the tension-compression curve and revealing the intrinsic properties of the tissue. With this method, we were able to measure the tensile (401±83 kPa for FS and 678±473 kPa for DL) and compressive (161±33 kPa for FS and 348±203 kPa for DL) moduli of the same engineered cartilage specimens. These moduli are comparable to values obtained from traditional methods, validating this technique for measuring the tensile and compressive properties of hydrogel-based constructs. This study shows that engineered cartilage exhibits tension-compression nonlinearity reminiscent of the native tissue, and that dynamic deformational loading can yield significantly higher tensile properties.

*351 Engineering Terrace, MC 8904 1210 Amsterdam Avenue Department of Biomedical Engineering Columbia University New York, NY 10027 Tel: (212) 854-6542 FAX: (212) 854-8725 cth6@columbia.edu.

Conflict of Interest No conflicts of interest to disclose.

Keywords

Introduction

Native articular cartilage exhibits low compressive Young's modulus (E_{-Y}; 0.1–1 MPa) (Wang et al., 2002; Park et al., 2004) relative to its high tensile Young's modulus (E_{+Y}; 3–6 MPa) (Kempson et al., 1968; Williamson et al., 2003; Williamson et al., 2003), which regulates the mechanical response of cartilage in unconfined compression (Cohen et al., 1998; Soulhat et al., 1999; Soltz and Ateshian, 2000; Huang et al., 2001; Huang et al., 2003; Chahine et al., 2004) and in contact configurations (Krishnan et al., 2004). Previous studies indicate that a high E_{+Y} combines with interstitial fluid pressurization to produce an elevated dynamic compressive modulus (G^*) at least 6X greater than E_{-Y} (Soltz and Ateshian, 2000; Park et al., 2003; Park and Ateshian, 2006). This mechanism arises because the high E_{+Y} of cartilage restricts lateral expansion of the tissue upon axial compression. Since the interstitial fluid cannot exude rapidly, the initial deformation must be nearly isochoric, occurring only if the interstitial fluid pressurizes considerably to help resist the compressive load. In order to distribute and absorb loads similar to native cartilage, engineered cartilage should exhibit similar tension-compression nonlinearity (TCN). Previous studies have demonstrated that chondrocyte seeded agarose constructs are capable of achieving native values for E_{-Y} and glycosaminoglycan (GAG) content (Kelly et al., 2006; Bian et al., 2009; Bian et al., 2009; Natoli et al., 2009; Natoli et al., 2009; Bian et al., 2010). While E_{-Y} and E_{+Y} have been independently analyzed previously, the role of TCN in developing engineered cartilage has not been addressed. Therefore, we adapted a method used previously to examine TCN in native cartilage (Chahine et al., 2004), which permits determination of E_{+Y} and E_{-Y} from a single specimen. Using this technique, E_{+Y} and E_{-Y} were found to be similar to values obtained from direct measurements using more conventional methods (Huang et al., 2001; Wang et al., 2002; Huang et al., 2003; Williamson et al., 2003; Williamson et al., 2003; Park et al., 2004; Huang et al., 2005). This technique uses osmotic swelling to place the sample in an initial state of tension. Small compressive displacement increments are then applied and the resultant loads are measured during the tissue's transition from tensile to compressive strains.

The underlying principle behind this technique stems from the fact that hydrated tissues possessing a fixed charge density swell and stiffen under hypotonic loading. Conversely, these tissues shrink and become softer under hypertonic loading via concomitant changes in Donnan osmotic pressure (Maroudas, 1976; Lai et al., 1991; Wang et al., 2002). Therefore, compressing swollen tissues allows for measurement of E_{+Y} when the *applied* compressive strain is smaller than the *true* tensile swelling strain of the solid matrix (Figure 1E). As the strain increases, the measured response yields E_{-Y}.

The objective of this study is to determine the TCN in engineered cartilage grown under free swelling (FS) or dynamically loaded (DL) cultures. We hypothesize that DL will improve both E_{+Y} and E_{-Y} of engineered cartilage compared to FS controls. Therefore, we acquired a spectrum of engineered cartilage moduli from tension to compression using compressive loading in the presence of osmotic swelling and report for the first time E_{+Y} and E_{-Y} of the same engineered cartilage specimen.

Materials and Methods

Sample Preparation and Tissue Culturing

Articular cartilage was harvested from adult canine knee joints. Three to five joints were used and cells were pooled from all joints, as previously described (Lima et al., 2007; Bian et al., 2010). Cartilage chunks were digested with 390 U/mL collagenase type VI (Sigma) for 11 hours with slight agitation. Isolated chondrocytes were passaged in DMEM containing 10%FBS, 10ng/mL PDGF, 1 ng/mL TGF-β1, 5 ng/mL FGF-2 and 1% antibiotics/antimycotics. Chondrocytes were seeded in 2% (w/v) agarose at 30×10^6 cells/mL and cast between parallel plates.

Cylindrical constructs (Ø4.0×2.3 mm) were cored and cultured in DMEM containing 50 µg/mL L-proline, 100 µg/mL sodium pyruvate, 1% ITS+ premix (BD Biosciences), 100 nM dexamethasone, 1% antibiotics/antimycotics, 50 µg/mL ascorbic acid, and 10 ng/mL TGF-β3 (R&D Systems). Constructs were maintained in FS culture for 14 days. After day 14, constructs were either cultured under DL conditions or maintained under FS conditions until day 42. For DL, a sinusoidal deformation with a magnitude of 10% surface-to-surface strain at a frequency of 1 Hz (5 days/week, 3 hours/day continuous) was applied, with an initial 2% tare strain.

Average Mechanical Properties

A custom unconfined compression device (Mauck et al., 2000) with rigid-impermeable glass loading platens and a 250-gram load cell (Honeywell Sensotec) was used to assess the E_{-Y} of the whole construct at days 0, 14, 28 and 42 (n=4–11). Before each test, the construct thickness and diameter were measured, specimens were equilibrated under a 0.02N tare load, and a 10% strain was applied at 0.05% strain/sec. E_{-Y} was calculated from the equilibrium stress and initial cross-sectional area. The average unconfined dynamic modulus (G*) was subsequently measured by superimposing a 2% sinusoidal strain at 1 Hz.

To establish whether E_{-Y} of engineered tissue was dependent on strain, immature bovine articular chondrocytes were harvested and used to create constructs, as described above. On days 0 and 42, these constructs were used in a series of stress-relaxation tests at 5%, 10%, 15%, and 20% strains (n=5). For comparison, freshly harvested explants were also tested.

Direct Tensile Testing of Agarose Constructs

Acellular constructs were cast as described above to test the tensile mechanical properties of 2% (w/v) agarose. Rectangular samples were cut from the slab (length=12 mm, width=3 mm, thickness=2.34 mm, n=7). Sandpaper grips were glued to the top and bottom edge of the sample and secured in metal grips that attached to the mechanical testing device (Instron). A quasi-static ramp was applied at a rate of 0.01%/s, and load and displacement data were recorded until failure. The tensile modulus was calculated as the slope of the stress-strain curve.

Tension-Compression Analysis

A custom glass-bottom device was mounted on the stage of an inverted microscope and used to mechanically test semi-cylindrical specimens (Wang et al., 2002; Wang et al., 2003; Chahine et al., 2004). Prior to testing, the thickness of each construct was measured, the constructs were halved, and each half was maintained in isotonic saline (Figure 1A). At days 0 (n=4) and 42 (n=4–6), the semi-cylindrical samples were tested in 0.015M NaCl (hypotonic saline) to determine TCN under conditions of maximal osmotic swelling (e.g., expansion of the collagen network) or 2M NaCl (hypertonic saline) to determine TCN under conditions where the contribution of osmotic swelling is minimal. As an additional control,

acellular constructs, cast with dark blue polystyrene microspheres (1×10^9 microspheres/mL; 0.88 μm diameter, Bangs Laboratories), were also analyzed in hypotonic saline to measure the TCN of 2% w/v agarose (n=4). The microspheres were used solely in cell-free constructs as fudicial markers to provide optical texture for DIC.

For testing, each semi-cylindrical sample was equilibrated for 1 hour in the appropriate saline solution containing LIVE/DEAD dyes (Invitrogen). The equilibrated thickness of the specimen was measured, initial images of the cross-section of the samples were acquired, and the samples were then compressed at nominal 2% strain increments, up to a final compression of 10–12% (Figure 1B). After each compression, samples were allowed to equilibrate for 15 minutes with images being acquired immediately before each subsequent compression (Figure 1C, D).

Optimized DIC was used to obtain accurate axial and lateral strains (Wang et al., 2002; Wang et al., 2003; Chahine et al., 2004; Kelly et al., 2006). The equilibrium normal stress was calculated from the measured load and the initial cross-sectional area of the constructs. The effective incremental Young's modulus (E_{Yi}) was calculated for each compression level (Figure 1E). E_{+Y} was defined as the highest E_{Yi} measured under initial compression in hypotonic saline, while E_{-Y} was defined as the nearly constant E_{Yi} obtained at higher compressive strains, an average of the values in the range of 8–10% compression. The incremental Poisson's ratio (ν_i) was also calculated as the negative ratio of the axial and lateral strains. After testing, the samples were processed for histology or weighed and stored at −20C for biochemical analysis.

Biochemical Analysis

Samples (n = 4–11) were thawed, lyophilized, and weighed dry and digested with 0.5 mg/mL proteinase K (Promega) in 50 mM Tris-buffered saline containing 1 mM EDTA, 1 mM iodoacetamide (Acros Organics). DNA content was quantified using a PicoGreen assay (Invitrogen) (McGowan et al., 2002) with lambda phage DNA standards. GAG was quantified using 1,9-dimethylmethylene blue (Sigma) dye-binding assay (McGowan et al., 2002), with shark chondroitin-6-sulfate (Sigma) standards. The digests were hydrolyzed in 5N HCl at 110°C for 16 hours and used to quantify the total collagen content via an orthohydroxyproline (OHP) colorimetric assay (Stegemann and Stalder, 1967) with bovine OHP (Sigma) standards. Collagen content was calculated by assuming a 1–10 OHP-to-collagen mass ratio (Stegemann and Stalder, 1967). The collagen and GAG contents were normalized to the construct wet weight, dry weight and DNA content.

Statistical Analysis

ANOVA (α=0.05) was used to determine significant differences (n=4–11). If significant changes were noted (p<0.05), Fisher's LSD post-hoc test was performed.

Results

Average Tissue Properties

At day 0, chondrocyte-seeded constructs exhibited strain-softening behavior between 5% and 20% compression (Figure 2A), where E_{-Y} decreased with increasing applied compressive strain. This behavior is typical of agarose hydrogels. By day 42, chondrocyte-seeded constructs (as well as the cartilage explants) exhibited E_{-Y} that remained nearly constant with increasing compressive strain over the tested range, indicative of a stiffer construct due to matrix elaboration and reflective of the diminished contribution of the agarose hydrogel to the overall stiffness.

E_{-Y} increased significantly over time in culture for both FS and DL constructs (p<0.005; Figure 2B, C). By day 28, E_{-Y} was significantly greater for DL constructs compared to FS controls (Figure 2B). DL did not yield significant differences in G* (Figure 2C).

The thickness, diameter, wet weight and dry weight of chondrocyte-seeded agarose hydrogels increased significantly over the 6-week culture period for both FS and DL constructs (p<0.005; Table 1), with significantly greater increases observed in FS constructs (p<0.05). Additionally, the water content decreased significantly over time in culture (p<0.0005); however, there were no significant differences with loading.

The biochemical content of the constructs increased significantly over time in culture (p<0.0005; Table 1 and Figure 3). The DNA content increased significantly over the 42-day culture period (p<0.0005), however, no significant differences with loading were observed. There were also no significant differences in the GAG content of FS and DL chondrocyte-seeded constructs. The collagen content was significantly higher in DL constructs than in FS constructs by day 42 when normalized to DNA or dry weight (p<0.05). No load-dependent differences in collagen content were observed when normalized to the construct wet weight. At day 42, GAG and collagens comprised a significant portion of the solid tissue components compared to day 0 (p<0.005; Figure 5). By day 42, GAGs and collagens accounted for 54% and 61% of the solid component (i.e. % normalized by dry weight) of FS and DL constructs, respectively.

At day 42, the distribution of GAG was similar in FS and DL constructs (compare Figure 3D to Figure 3E). However, more labeling of collagen was observed in the central regions of DL constructs (Figure 3F) compared to FS controls (Figure 3G).

Tension-Compression Nonlinearity

The effects of salt concentration on the thickness and material properties of chondrocyte-seeded constructs are presented in Table 2. The samples were first mechanically tested whole to yield average construct properties, and then allowed to recover for 60 minutes in the appropriate saline solution prior to testing in the custom-built microscope-mounted testing rig (Figure 1). Similar intergroup differences in tissue dimensions were observed before bulk testing and after recovery in saline (compare Table 1 and Table 2). Additionally, the thickness of DL constructs increased significantly in hypotonic saline (p<0.05), which corresponds to a 3% increase in thickness. There was a 2% increase in thickness observed for the FS controls, however, this difference was not significant. In hypertonic saline, the FS and DL samples shrunk by 4% and 3% (p<0.05), respectively. In all cases, DL samples showed significantly lower temporal increases in construct dimensions than FS controls (p<0.05).

The effects of salt concentration on the apparent E_{Yi} of acellular and chondrocyte-seeded constructs are shown in Figures 4A, 5 and 7A and in Table 2. Strain-softening behavior was observed in day 0 and acellular samples. There was no dependence on salt concentration, which is consistent with the uncharged nature of agarose hydrogels. Here, E_{+Y} and E_{-Y} obtained for day 0 and acellular constructs were 28–40 kPa and 8–10 kPa, respectively. Direct measurement of acellular agarose yielded similar results (E_{+Y} = 39 kPa and E_{-Y} = 11 kPa) (Figure 4A Inset).

At day 42, FS and DL constructs exhibited similar changes in the apparent E_{Yi} in response to changes in salt concentration and applied strain (Figure 5). Here, the constructs are placed in a state of tension via applied hypotonic loading; therefore, E_{Yi} measured at low applied strain (below the swelling strain of the constructs) represents E_{+Y} of the constructs. As the construct is compressed, the tissue transitions from a state of tension to compression,

permitting the examination of TCN in these constructs. At both salt concentrations, the apparent E_{Yi} was highest at the lowest applied strain and decreased with increasing applied strain. Overall, the measured apparent E_{Yi} increased with decreasing salt concentration. In the hypotonic state, DL constructs exhibited significantly higher apparent E_{Yi} than FS constructs (Figure 6A). No significant differences in the apparent E_{Yi} were observed in hypertonic saline (Figure 6B, C).

In hypotonic saline, the apparent E_{+Y} (Table 2) was obtained at the lowest strain increment (401 kPa for FS and 678 kPa for DL), which was significantly higher than hypertonic saline values (46 kPa for FS and 35 kPa for DL; p<0.05). Additionally, at each salt concentration, the apparent E_{+Y} of DL constructs was significantly higher than that of the FS controls (p<0.05). At high strain, the apparent E_{-Y} of FS constructs was similar in hypotonic and hypertonic saline. However, for DL constructs, the apparent E_{-Y} was significantly greater for constructs in hypotonic saline compared to hypertonic saline (p<0.05).

The effects of salt concentration on the apparent ν_i of acellular and chondrocyte-seeded constructs are shown in Figures 4B, 6 and 7B. At day 0, ν_i remained constant as the incremental strain was increased and were similar at all saline concentrations (Figure 4B). At day 42, FS and DL constructs exhibited disparate changes in ν_i in response to changes in salt concentration and applied strain (Figure 6). For FS constructs tested in hypotonic saline, ν_i was high at low strain and decreased at higher applied strain to a steady-state value. In hypertonic saline, ν_i remained constant across all applied strains, similar to the ν_i obtained at higher applied strain in hypotonic saline. For DL, when tested in hypotonic saline, ν_i was initially low, compared to FS controls, but decreased slightly as the applied strain was increased to a steady-state value. In hypertonic saline, ν_i did not vary with increased applied strain. Here, ν_i was similar to the values measured in hypotonic saline at higher applied strains. Furthermore, in hypertonic saline, similar ν_i was obtained for both FS and DL constructs.

The data in Figures 5 and 6 were combined using the construct's swelling strains (Tables 2) to generate TCN plots for both E_{Yi} and ν_i (Figure 7). Under these conditions, E_{+Y} of both FS and DL constructs were significantly higher in tension, decreasing exponentially as the constructs transition to purely compressive conditions (Figure 7A; R^2=0.98–0.99 p<0.05). Additionally, DL constructs exhibited significantly higher E_{+Y} compared to FS controls (p<0.05). These trends were comparable to those observed for native cartilage (Figure 7A Inset).

In FS constructs, ν_i was significantly higher when the constructs were in tension but decreased exponentially as the constructs transitioned into purely compressive conditions (Figure 7B; R^2 = 0.87; p<0.05). For DL constructs, ν_i exhibited a slight but exponential decrease as the tissue transitioned from tensile to compressive conditions (R^2=0.60). Additionally, ν_i of DL constructs was significantly lower than FS controls when the constructs were placed in tension (p<0.05). ν_i showed similar trends to native cartilage (Figure 7B Inset), i.e. decreased nonlinearly with increased strain, however under tensile strain, ν_i was higher than i native tissue.

Discussion

In this study, osmotic swelling and uniaxial compressive loading were used to determine tensile and compressive responses within the same chondrocyte-seeded agarose constructs. Using the general framework of porous media mechanics and Donnan equilibrium theory (Overbeek, 1956; Maroudas, 1976; Grodzinsky, 1983; Lanir, 1987; Lai et al., 1991; Basser et al., 1998; Wang et al., 2002; Ateshian et al., 2004; Chahine et al., 2004; Wilson et al.,

2007), it is apparent that bathing native or engineered cartilage in solutions of greater salt concentration will result in a decreased contribution of osmotic pressure to the effective tissue material responses (due to increased shielding of the fixed charge density arising from GAGs). Likewise, bathing native or engineered cartilage in hypotonic solution results in tissue swelling (relative to isotonic dimensions) and stiffening. Tissue swelling is a manifestation of the expansion of the fibrillar collagen network (e.g., recruitment of collagen fibers extended beyond their toe-region) to balance the increase in Donnan osmotic pressure resulting from the fixed charge density associated with the GAGs (Maroudas, 1976).

While the E_{-Y} of 2% agarose is in a typical range of 5–15 kPa (Figure 4 inset), tensile testing yielded E_{+Y} of 39 kPa, similar to previously reported values (Huang et al., 2008). Although agarose does not exhibit swelling or shrinking in response to salt solutions, there is observable strain-softening in response to greater levels of applied compression. The initially higher E_{Yi} at very low applied compression, similar to the measured E_{+Y} determined from conventional testing, is thought to arise from residual stresses of the polymer that place the hydrogel in a swollen state during gelation (Amici et al., 2000; Normand et al., 2000). As this swollen state is overcome, compressive properties are exhibited. Since E_{-Y} and E_{+Y} of mature engineered tissues are more than an order of magnitude greater than agarose, the hydrogel scaffold contributes minimally to the mechanical behavior of the mature engineered tissues.

The results of this study showed that testing of mature (day 42) engineered cartilage in hypertonic saline significantly reduced the apparent E_{Yi} of constructs relative to hypertonic conditions but not to day 0 levels, which were consistent with data obtained for native cartilage (Chahine et al., 2005). In contrast, for immature (day 0) and acellular constructs, no differences were observed at various salt concentrations (Figure 4A). These results confirm that the observed effects of salt concentration can be attributed to the charged GAG species accumulated in the mature engineered cartilage over time (Ehrlich et al., 1998; Chahine et al., 2005). Cell swelling may contribute to the tensing of the fibrillar collagen network, however previous results indicate the ECM acts to limit cell expansion (Lee and Bader, 1995; Knight et al., 1998). As such, the measured properties with hypertonic saline reflect the intrinsic material properties of the engineered cartilage without the contribution of Donnan osmotic pressure.

When the matrix is in a state of tension the measured stiffness represents E_{+Y}, the highest modulus measured under initial compression in hypotonic saline. The results of this study indicate that tissue growth of chondrocyte-seeded agarose constructs leads to an increase in E_{+Y}. At day 42, E_{+Y} measured in hypotonic saline ranged from an average of 0.40 MPa for FS constructs to 0.68 MPa for DL constructs. E_{+Y} ranging from 0.2 to 5 MPa has been reported for engineered cartilage (Gemmiti and Guldberg, 2006; Huang et al., 2008; Bian et al., 2009; Gemmiti and Guldberg, 2009; Natoli et al., 2009; Natoli et al., 2009; Moutos and Guilak, 2010; Natoli et al., 2010; Eleswarapu et al., 2011; Eleswarapu and Athanasiou, 2012; Huang et al., 2012). In fact, previous data from our laboratory for constructs cultured under similar conditions found similar tensile properties (0.2 MPa for Bian's CONT versus 0.4 MPa for FS) (Bian et al., 2009). Those values are consistent with E_{+Y} observed in this study at day 42. As with native cartilage, the measured E_{Yi} decreased with increasing salt concentration, since the concomitant reduction in swelling pressure also reduced the swelling strain, thereby shifting the FS initial configuration on the TCN curve to the left (Figure 1; (Chahine et al., 2005)). Furthermore, increasing the swelling strain by further decreasing the bathing media osmolarity would be anticipated to yield a higher measured E_{Yi}, thereby shifting the TCN curve to the right. We chose 0.015M NaCl, because it allows for sufficient tissue swelling without causing the tissue to burst apart.

This method allows for the analysis of local material properties of the constructs, however, due to manuscript page limitations, this data was not included in the manuscript. Spatial variation in E_{+Y} was similar to those previously reported for E_{-Y}, that is the edges of the constructs (i.e., axial faces) were stiffer compared to the middle with DL exhibiting stiffer middle compared to FS controls (Kelly et al., 2006).

The results of this study confirmed our previous observation that DL yielded lower ν than FS culture, which is expected if DL constructs have higher E_{+Y} than FS controls (Kelly et al., 2006). The observed increases in tensile ν_i of FS constructs over native values emphasize the importance of E_{+Y} on proper functioning of cartilaginous tissues (Figure 7B). For DL constructs, ν_i was in the range observed for native cartilage. Higher swelling strains may be required to fully elucidate the effects of tensile strain on ν_i.

When comparing FS and DL cultures, it is found that the biochemical composition evolves similarly for both groups at most time points, except for day 42, where the collagen content is greater in DL group when normalized to the DNA or dry weight (Figure 3C & Table 1). The mechanical response of the tissues exhibit significant differences on day 42 for E_{-Y} (Figure 2B); however, no significant difference in G^* was observed (Figure 2C). E_{+Y} measured from the osmotic swelling experiments shows a significantly higher value in DL group (Figure 4C). We have previously shown that DL produces constructs with a more organized matrix than those grown in FS culture. More specifically, in DL constructs, the collagen fibers were shown to be aligned transversely to the direction of loading with increased type II and IX collagen (Kelly et al., 2004; Kelly et al., 2006), which may have contributed to the increased E_{+Y}.

The best results from these studies reveal engineered cartilage with E_{-Y} and GAG content similar to those of native cartilage; however, G^* (~10–30% of native), E_{+Y} (~15–25%) and collagen (~24–48%) are a fraction of the native values (Chahine et al., 2004; Huang et al., 2005). Low collagen content and its effect on engineered cartilage material properties remains a major challenge in cartilage tissue engineering (Riesle et al., 1998; Mauck et al., 2000; Mauck et al., 2002; Williamson et al., 2003; Kelly et al., 2004; Gemmiti and Guldberg, 2006; Kelly et al., 2006).

Here, hypotonic and hypertonic conditions were used as a methodological tool to examine TCN in these constructs. For the first time, we are able to determine E_{-Y} and E_{+Y} of engineered cartilage using applied compressive loading without the need to prepare multiple specimens or conduct multiple experiments. The resolution of optical strain measurements makes it possible to examine the transition from tension to compression, producing a clearer understanding of the disparate material properties of DL and FS constructs. More complete characterizations of the material properties of engineered cartilage can improve critical assessments of the efficacy of tissue engineering approaches for producing functional tissues for articular cartilage repair and replacement.

Acknowledgments

References

Amici E, Clark AH, Normand V, Johnson NB. Interpenetrating network formation in gellan--agarose gel composites. Biomacromolecules. 2000; 1:721–729. [PubMed: 11710203]

Ateshian GA, Chahine NO, Basalo IM, Hung CT. The correspondence between equilibrium biphasic and triphasic material properties in mixture models of articular cartilage. J Biomech. 2004; 37:391–400. [PubMed: 14757459]

Basser PJ, Schneiderman R, Bank RA, Wachtel E, Maroudas A. Mechanical properties of the collagen network in human articular cartilage as measured by osmotic stress technique. Arch Biochem Biophys. 1998; 351:207–219. [PubMed: 9515057]

Bian L, Angione SL, Ng KW, Lima EG, Williams DY, Mao DQ, Ateshian GA, Hung CT. Influence of decreasing nutrient path length on the development of engineered cartilage. Osteoarthritis Cartilage. 2009; 17:677–685. [PubMed: 19022685]

Bian L, Crivello KM, Ng KW, Xu D, Williams DY, Ateshian GA, Hung CT. Influence of temporary chondroitinase ABC-induced glycosaminoglycan suppression on maturation of tissue-engineered cartilage. Tissue Eng Part A. 2009; 15:2065–2072. [PubMed: 19196151]

Bian L, Fong JV, Lima EG, Stoker AM, Ateshian GA, Cook JL, Hung CT. Dynamic mechanical loading enhances functional properties of tissue-engineered cartilage using mature canine chondrocytes. Tissue Eng Part A. 2010; 16:1781–1790. [PubMed: 20028219]

Chahine NO, Chen FH, Hung CT, Ateshian GA. Direct measurement of osmotic pressure of glycosaminoglycan solutions by membrane osmometry at room temperature. Biophys J. 2005; 89:1543–1550. [PubMed: 15980166]

Chahine NO, Wang CC, Hung CT, Ateshian GA. Anisotropic strain-dependent material properties of bovine articular cartilage in the transitional range from tension to compression. J Biomech. 2004; 37:1251–1261. [PubMed: 15212931]

Cohen B, Lai WM, Mow VC. A transversely isotropic biphasic model for unconfined compression of growth plate and chondroepiphysis. J Biomech Eng. 1998; 120:491–496. [PubMed: 10412420]

Ehrlich S, Wolff N, Schneiderman R, Maroudas A, Parker KH, Winlove CP. The osmotic pressure of chondroitin sulphate solutions: experimental measurements and theoretical analysis. Biorheology. 1998; 35:383–397. [PubMed: 10656048]

Eleswarapu SV, Athanasiou KA. TRPV4 channel activation improves the tensile properties of self-assembled articular cartilage constructs. Acta Biomater. 2012

Eleswarapu SV, Chen JA, Athanasiou KA. Temporal assessment of ribose treatment on self-assembled articular cartilage constructs. Biochem Biophys Res Commun. 2011; 414:431–436. [PubMed: 21971556]

Gemmiti CV, Guldberg RE. Fluid flow increases type II collagen deposition and tensile mechanical properties in bioreactor-grown tissue-engineered cartilage. Tissue Eng. 2006; 12:469–479. [PubMed: 16579680]

Gemmiti CV, Guldberg RE. Shear stress magnitude and duration modulates matrix composition and tensile mechanical properties in engineered cartilaginous tissue. Biotechnol Bioeng. 2009; 104:809–820. [PubMed: 19591192]

Grodzinsky AJ. Electromechanical and physicochemical properties of connective tissue. Crit Rev Biomed Eng. 1983; 9:133–199. [PubMed: 6342940]

Huang AH, Baker BM, Ateshian GA, Mauck RL. Sliding contact loading enhances the tensile properties of mesenchymal stem cell-seeded hydrogels. Eur Cell Mater. 2012; 24:29–45. [PubMed: 22791371]

Huang AH, Yeger-McKeever M, Stein A, Mauck RL. Tensile properties of engineered cartilage formed from chondrocyte- and MSC-laden hydrogels. Osteoarthritis Cartilage. 2008; 16:1074–1082. [PubMed: 18353693]

Huang CY, Mow VC, Ateshian GA. The role of flow-independent viscoelasticity in the biphasic tensile and compressive responses of articular cartilage. J Biomech Eng. 2001; 123:410–417. [PubMed: 11601725]

Huang CY, Soltz MA, Kopacz M, Mow VC, Ateshian GA. Experimental verification of the roles of intrinsic matrix viscoelasticity and tension-compression nonlinearity in the biphasic response of cartilage. J Biomech Eng. 2003; 125:84–93. [PubMed: 12661200]

Huang CY, Stankiewicz A, Ateshian GA, Mow VC. Anisotropy, inhomogeneity, and tension-compression nonlinearity of human glenohumeral cartilage in finite deformation. J Biomech. 2005; 38:799–809. [PubMed: 15713301]

Kelly TA, Ng KW, Wang CC, Ateshian GA, Hung CT. Spatial and temporal development of chondrocyte-seeded agarose constructs in free-swelling and dynamically loaded cultures. J Biomech. 2006; 39:1489–1497. [PubMed: 15990101]

Kelly TA, Wang CC, Mauck RL, Ateshian GA, Hung CT. Role of cell-associated matrix in the development of free-swelling and dynamically loaded chondrocyte-seeded agarose gels. Biorheology. 2004; 41:223–237. [PubMed: 15299255]

Kempson GE, Freeman MA, Swanson SA. Tensile properties of articular cartilage. Nature. 1968; 220:1127–1128. [PubMed: 5723609]

Knight MM, Lee DA, Bader DL. The influence of elaborated pericellular matrix on the deformation of isolated articular chondrocytes cultured in agarose. Biochim Biophys Acta. 1998; 1405:67–77. [PubMed: 9784610]

Krishnan R, Kopacz M, Ateshian GA. Experimental verification of the role of interstitial fluid pressurization in cartilage lubrication. J Orthop Res. 2004; 22:565–570. [PubMed: 15099636]

Lai WM, Hou JS, Mow VC. A triphasic theory for the swelling and deformation behaviors of articular cartilage. J Biomech Eng. 1991; 113:245–258. [PubMed: 1921350]

Lanir Y. Biorheology and fluid flux in swelling tissues, II. Analysis of unconfined compressive response of transversely isotropic cartilage disc. Biorheology. 1987; 24:189–205. [PubMed: 3651591]

Lee DA, Bader DL. The development and characterization of an in vitro system to study strain-induced cell deformation in isolated chondrocytes. In Vitro Cell Dev Biol Anim. 1995; 31:828–835. [PubMed: 8826085]

Lima EG, Bian L, Ng KW, Mauck RL, Byers BA, Tuan RS, Ateshian GA, Hung CT. The beneficial effect of delayed compressive loading on tissue-engineered cartilage constructs cultured with TGF-beta3. Osteoarthritis Cartilage. 2007; 15:1025–1033. [PubMed: 17498976]

Maroudas AI. Balance between swelling pressure and collagen tension in normal and degenerate cartilage. Nature. 1976; 260:808–809. [PubMed: 1264261]

Mauck RL, Seyhan SL, Ateshian GA, Hung CT. Influence of seeding density and dynamic deformational loading on the developing structure/function relationships of chondrocyte-seeded agarose hydrogels. Ann Biomed Eng. 2002; 30:1046–1056. [PubMed: 12449765]

Mauck RL, Soltz MA, Wang CC, Wong DD, Chao PH, Valhmu WB, Hung CT, Ateshian GA. Functional tissue engineering of articular cartilage through dynamic loading of chondrocyte-seeded agarose gels. J Biomech Eng. 2000; 122:252–260. [PubMed: 10923293]

McGowan KB, Kurtis MS, Lottman LM, Watson D, Sah RL. Biochemical quantification of DNA in human articular and septal cartilage using PicoGreen and Hoechst 33258. Osteoarthritis Cartilage. 2002; 10:580–587. [PubMed: 12127839]

Moutos FT, Guilak F. Functional properties of cell-seeded three-dimensionally woven poly(epsilon-caprolactone) scaffolds for cartilage tissue engineering. Tissue Eng Part A. 2010; 16:1291–1301. [PubMed: 19903085]

Natoli RM, Responte DJ, Lu BY, Athanasiou KA. Effects of multiple chondroitinase ABC applications on tissue engineered articular cartilage. J Orthop Res. 2009; 27:949–956. [PubMed: 19123232]

Natoli RM, Revell CM, Athanasiou KA. Chondroitinase ABC treatment results in greater tensile properties of self-assembled tissue-engineered articular cartilage. Tissue Eng Part A. 2009; 15:3119–3128. [PubMed: 19344291]

Natoli RM, Skaalure S, Bijlani S, Chen KX, Hu J, Athanasiou KA. Intracellular Na(+) and Ca(2+) modulation increases the tensile properties of developing engineered articular cartilage. Arthritis Rheum. 2010; 62:1097–1107. [PubMed: 20131245]

Normand V, Lootens DL, Amici E, Plucknett KP, Aymard P. New insight into agarose gel mechanical properties. Biomacromolecules. 2000; 1:730–738. [PubMed: 11710204]

Overbeek JT. The Donnan equilibrium. Prog Biophys Biophys Chem. 1956; 6:57–84. [PubMed: 13420188]

Park S, Ateshian GA. Dynamic response of immature bovine articular cartilage in tension and compression, and nonlinear viscoelastic modeling of the tensile response. J Biomech Eng. 2006; 128:623–630. [PubMed: 16813454]

Park S, Hung CT, Ateshian GA. Mechanical response of bovine articular cartilage under dynamic unconfined compression loading at physiological stress levels. Osteoarthritis Cartilage. 2004; 12:65–73. [PubMed: 14697684]

Park S, Krishnan R, Nicoll SB, Ateshian GA. Cartilage interstitial fluid load support in unconfined compression. J Biomech. 2003; 36:1785–1796. [PubMed: 14614932]

Riesle J, Hollander AP, Langer R, Freed LE, Vunjak-Novakovic G. Collagen in tissue-engineered cartilage: types, structure, and crosslinks. J Cell Biochem. 1998; 71:313–327. [PubMed: 9831069]

Soltz MA, Ateshian GA. A Conewise Linear Elasticity mixture model for the analysis of tension-compression nonlinearity in articular cartilage. J Biomech Eng. 2000; 122:576–586. [PubMed: 11192377]

Soulhat J, Buschmann MD, Shirazi-Adl A. A fibril-network-reinforced biphasic model of cartilage in unconfined compression. J Biomech Eng. 1999; 121:340–347. [PubMed: 10396701]

Stegemann H, Stalder K. Determination of hydroxyproline. Clin Chim Acta. 1967; 18:267–273. [PubMed: 4864804]

Wang CC, Chahine NO, Hung CT, Ateshian GA. Optical determination of anisotropic material properties of bovine articular cartilage in compression. J Biomech. 2003; 36:339–353. [PubMed: 12594982]

Wang CC, Deng JM, Ateshian GA, Hung CT. An automated approach for direct measurement of two-dimensional strain distributions within articular cartilage under unconfined compression. J Biomech Eng. 2002; 124:557–567. [PubMed: 12405599]

Wang CC, Guo XE, Sun D, Mow VC, Ateshian GA, Hung CT. The functional environment of chondrocytes within cartilage subjected to compressive loading: a theoretical and experimental approach. Biorheology. 2002; 39:11–25. [PubMed: 12082263]

Williamson AK, Chen AC, Masuda K, Thonar EJ, Sah RL. Tensile mechanical properties of bovine articular cartilage: variations with growth and relationships to collagen network components. J Orthop Res. 2003; 21:872–880. [PubMed: 12919876]

Williamson AK, Masuda K, Thonar EJ, Sah RL. Growth of immature articular cartilage in vitro: correlated variation in tensile biomechanical and collagen network properties. Tissue Eng. 2003; 9:625–634. [PubMed: 13678441]

Wilson CG, Palmer AW, Zuo F, Eugui E, Wilson S, Mackenzie R, Sandy JD, Levenston ME. Selective and non-selective metalloproteinase inhibitors reduce IL-1-induced cartilage degradation and loss of mechanical properties. Matrix Biol. 2007; 26:259–268. [PubMed: 17174540]
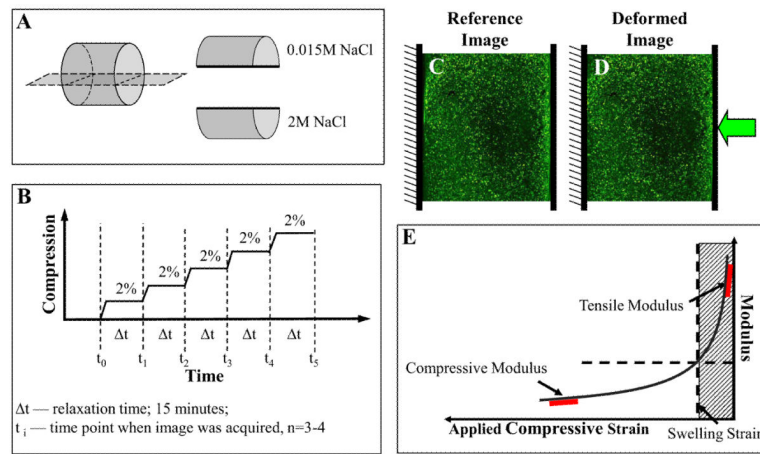
Figure 1.
A. Prior to osmotic testing the semi-cylindrical samples were equilibrated in the appropriate saline solution (Solution A and Solution B). The order of testing was rotated to prevent bias from multiple testing of the same semi-cylindrical sample. *B.* For each test, the semi-cylinder was loading into the microscope testing device and compressed at 2% increment to a final compression of 10–12% and allowed to equilibrate for 15 minutes between each compression. Images were acquired prior to each compression. *C, D.* Images of typical construct before (C) and after (D) compression. *E.* Schematic tension-compression curve: By controlling the osmolarity of the bathing fluid we can swell or shrink a test sample along its tension-compression curve. By then applying a compressive load to a swollen construct and comparing its properties to an unswollen construct we can extract its tensile modulus under compression without special grips. Hatched region represents region where specimen is under tension.
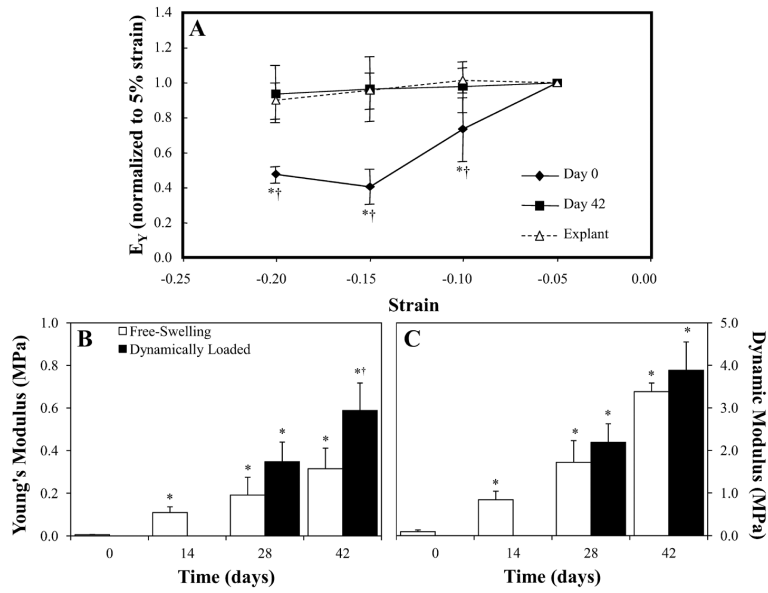
Figure 2.
A. The Young's modulus (E_Y) of chondrocyte-seeded constructs tested at days 0 and 42, in isotonic (0.15M NaCl) saline at 5% strain intervals and normalized to 5% strain values. Immature bovine cartilage explants were tested as an additional control. * $p<0.05$ versus all other strain levels; † $p<0.05$ versus day 42 constructs and cartilage explants (n=5). **B, C.** Young's modulus (B; E_Y) and dynamic modulus at 1.0 Hz (C; G^*) of free-swelling (FS) and dynamically loaded (DL) constructs (n=5–6) over a 42-day culture period. * $p<0.005$ versus day 0; † $p<0.05$ versus FS controls.
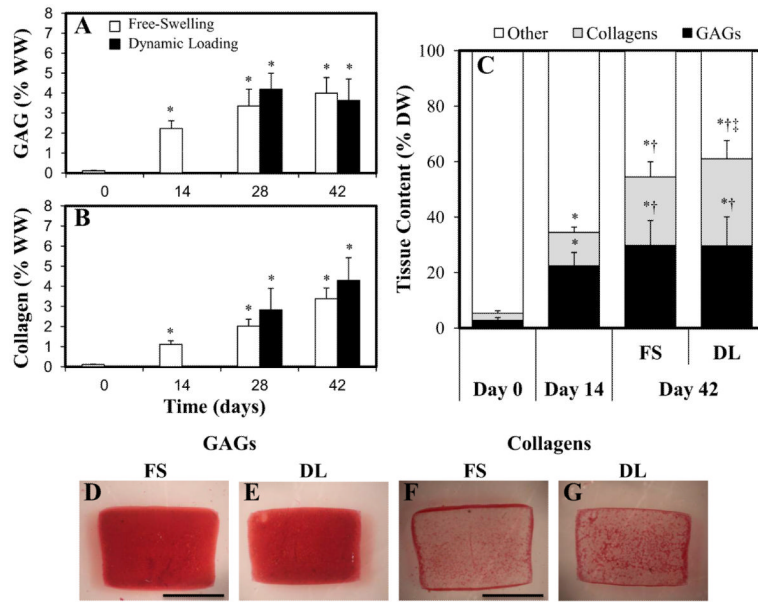
Figure 3.
A, B. GAG (A) and collagen (B) contents (normalized to the wet weight (WW) of the constructs) of free-swelling (FS) and dynamically loaded (DL) constructs over a 42-day culture period (n=5–11). * p<0.005 versus day 0; † p<0.05 versus FS controls. ***C.*** Biochemical content normalized to the dry weight (DW) of FS and DL constructs over a 42-day culture period (n=5–11). ***D–G.*** Safranin O (GAGs) and Picrosirius Red (collagens) staining of FS and DL constructs at day 42.
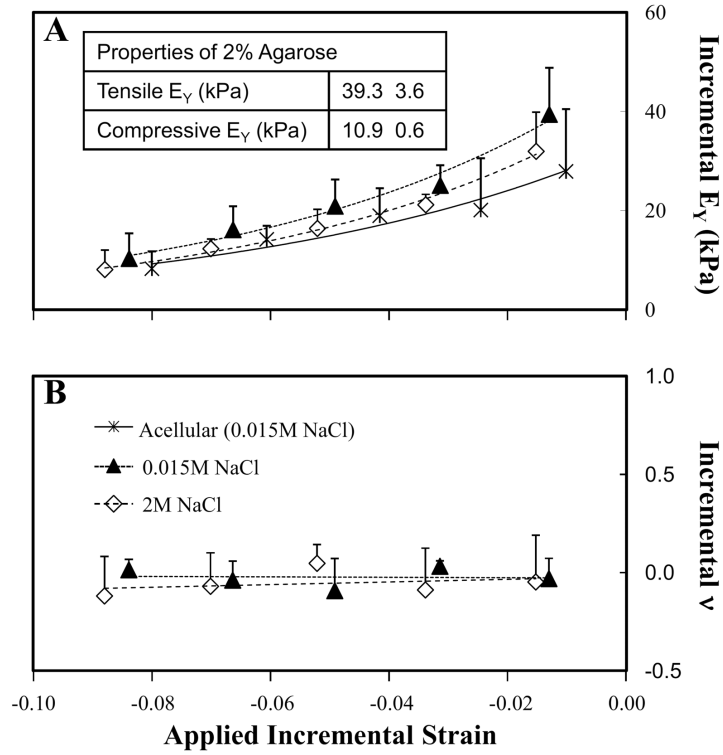
Figure 4.
A. Incremental Young's modulus (E_{Yi}) of acellular and day 0 chondrocyte-seeded agarose constructs tested in hypotonic (0.015M NaCl) and hypertonic (2M NaCl) saline (n=4). ***Inset.*** Compressive and tensile EY of 2% agarose obtained from direct measurements (n=7). **B**, Incremental Poisson's ratio (ν_i) of day 0 chondrocyte-seeded agarose constructs tested in hypotonic (0.015M NaCl) and hypertonic (2M NaCl) saline (n=4).
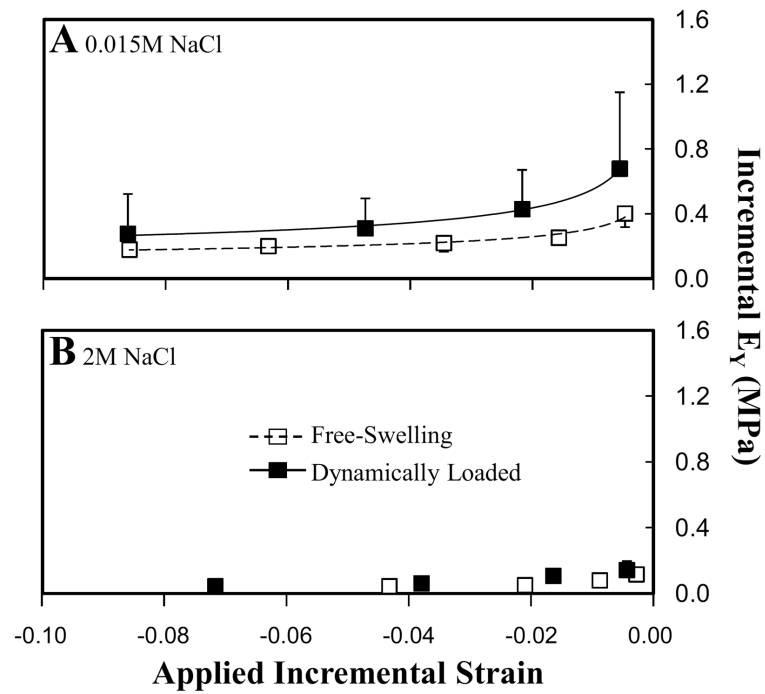
Figure 5.
Incremental Young's modulus (E_{Yi}) of free-swelling (FS) and dynamically loaded (DL) chondrocyte-seeded agarose constructs tested in hypotonic (A; 0.015M NaCl) and hypertonic (B; 2M NaCl) saline on day 42 (n=4–6). * $p<0.05$ versus free FS, † $p<0.05$ versus higher strain values $p<0.05$; § $p<0.05$ versus >3% strain values.
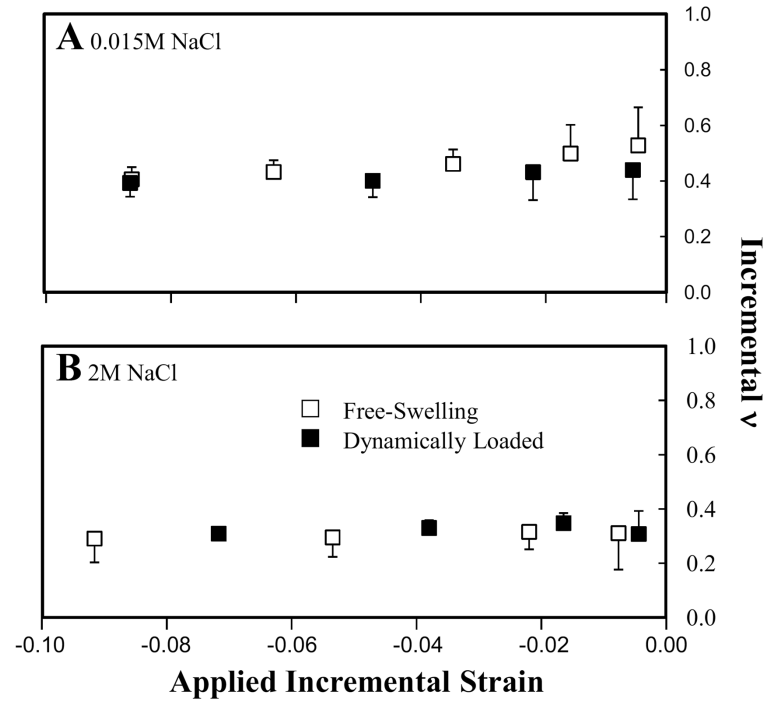
Figure 6.
Incremental Poisson's ratio (ν_i) of free-swelling (FS) and dynamically loaded (DL) chondrocyte-seeded agarose constructs tested in hypotonic (A; 0.015M NaCl) and hypertonic (B; 2M NaCl) saline on day 42 (n=4–6). * $p < 0.05$ versus FS, † $p < 0.05$ versus higher strain values $p < 0.05$; § $p < 0.05$ versus >3% strain values.
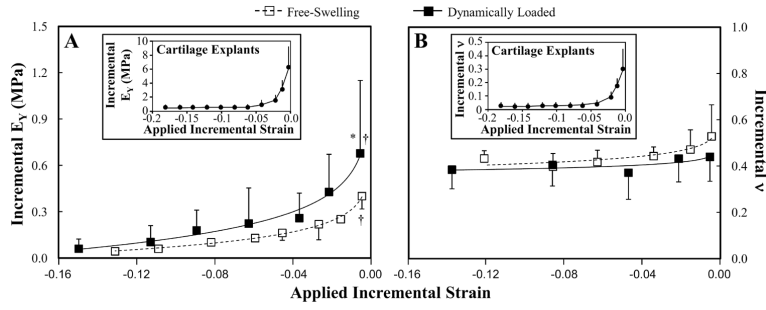
Figure 7.
A, B. Tension-compression nonlinearity plots highlighting differences in the incremental Young's modulus (A; E_{Yi}) and incremental Poisson's ratio (B; ν_i) of free-swelling (FS) and dynamically loaded (DL) chondrocyte-seeded agarose constructs tested in hypotonic (0.015M NaCl) and hypertonic (2M NaCl) saline on day 42 (n=4–6). * $p < 0.05$ versus FS, † $p < 0.05$ versus higher strain values; § $p < 0.05$ versus >3% strain values. The data was curvefitted to show the overall trends. In all cases exponential functions yielded best-fits (E_{Yi} FS $R^2 = 0.99$; E_{Yi} DL $R^2 = 0.98$; ν FS $R^2 = 0.87$; ν DL $R^2 = 0.60$). *Insets.* Tension-compression nonlinearity plots illustrating Young's modulus (A; E_{Yi}) and incremental Poisson's ratio (B; ν_i) of cartilage explants (in the depth direction; n=8).

Table 1

The bulk morphological and biochemical properties of chondrocyte-seeded agarose hydrogels grown in free-swelling (FS) and dynamically loaded (DL) cultures over a 6-week period (for day 0, n=4–5; for day 42, n=6–11; mean ± standard deviation).

	Day 0	Day 42	
		FS	DL
Thickness (mm)	2.34±0.02	2.72±0.10*	2.59±0.10*†
Diameter (mm)	3.76±0.04	4.12±0.15*	4.09±0.12*
Wet Weight (mg)	25.3±0.8	39.5±10.0*	37.4±6.3*†
Dry Weight (mg)	1.1±0.3	5.4±1.6*	4.8±0.5*†
Water Content (%)	95.5±1.2	86.7±2.7*	86.9±3.2*
DNA (% wet weight)	0.016±0.004	0.024±0.004*	0.022±0.005*
GAG (% wet weight)	0.1±0.0	4.0±0.8*	3.6±1.1*
Collagen (% wet weight)	0.1±0.0	3.4±0.5*	4.8±1.1*
GAG/DNA (μg/μg)	7.7±1.8	17.1±4.1*	15.8±4.5*
Collagen/DNA (μg/μg)	7.4±2.3	12.3±2.2*	18.5±4.0*†

Note that the thickness and diameter presented here were measured prior to any testing.

* represents significant differences versus day 0 ($p < 0.0005$);

† represents significant differences versus FS controls ($p < 0.05$).

Table 2

The effects of osmotic loading were determined for free-swelling (FS) and dynamically loaded (DL) constructs that were tested in 2M or 0.015M salt solution (n=4–5, mean ± standard deviation).

		Day 0	Day 42	
			FS	DL
Thickness (mm)	**0.015M NaCl**	2.35±0.02	2.71±0.05 *	2.65±0.05 *§
	2M NaCl	2.33±0.03	2.55±0.08 *	2.34±0.06 *†
Diameter (mm)	**0.015M NaCl**	4.04±0.04	4.11±0.19 *‡	4.19±0.10 *†§‡
	2M NaCl	3.97±0.10	3.99±0.09 *	3.99±0.12 *†
Swelling Strain (normalized to 0.15M NaCl)	**0.015M NaCl**	0.01±0.01	0.02±0.01	0.03±0.02
	2M NaCl	−0.01±0.01	−0.04±0.02	−0.03±0.02
Maximum Incremental Young's Modulus (kPa)	**0.015M NaCl**	39±9	401±83 *§	678±473 *†§
	2M NaCl	32±8	115±15 *	141±55 *
Steady-State Incremental Young's Modulus (kPa)	**0.015M NaCl**	5±2	161±33 *	348±203 *†§
	2M NaCl	5±1	46±9 *‡	35±16 *

Note that the thickness and diameter presented here were measure after equilibration in the appropriate saline solution, but prior to microscopic mechanical testing.

* represents significant differences versus day 0 constructs (p<0.05);

† represents significant differences versus FS constructs (p<0.05);

§ represents significant differences versus 2M NaCl values (p<0.05).